THE GROWTH MECHANISM IN SELF-ASSEMBLY NANOSTRUCTURES OF SILICON/SILICON DIOXIDE INTERFACE

FATIMA ALDAW IDREES

A thesis submitted in fulfilment
of the requirements for the award of the degree of
Doctor of Philosophy (Physics)

Faculty of Science
Universiti Teknologi Malaysia

FEBRUARY 2013

Thanks for "ALLAH" guide me to succeed my work,

and thanks for my parents, siblings, nephews and my friends,

thanks for encourage me towards academic with pleasant experience.

ACKNOWLEDGEMENTS

I am very pleased for those who support me to write this thesis. First of all, I would like to express my sincerest appreciation to my supervisor, Prof. Dr. Samsudi Sakrani, and my co-supervisor, Associate Prof. Dr. Zulkafli Othaman for their advice and encouragement.

My further appreciation to my research “QuaSR” group members who had supported me to success this project. Their assist and encouragement are inestimably important. Next, I like to thanks all the lab assistants and science officers from Physics Department of Science Faculty and Ibnu Sina Institute for Fundamental Science Studies, UTM for their assist during my research Mr. Imam Sumpono, Mr. Mohamad Nazri and Md. Wani from Ibnu Sina Institute, UTM, and Md. Norhayah, Md. Junidah.

Also, I wish to thank the Ministry of Higher Education for providing part of the financial support through FRSG funding 78416.

Last but not least, I would like to thank my dear parents, family members, my sister Hala, brother Mohamed, nephews Ahmed and Awab for supporting me to pass the troubles during my work.

ABSTRACT

Silicon nanodots is a common zero-dimensional nanomaterial investigated for single-electron device applications in integrated circuits. The current study attempts to look into the ever-popular silicon self-assembly nanodot grown on different substrates, with emphasis on its growth theory and characterizations. Discrepancy in its growth theories has led to misunderstanding and therefore innovative approaches are presented in this study to clarify and resolve the existing problems. A radio-frequency magnetron sputtering method was used for Silicon nanodots deposition, with the following conditions: argon gas flow rate 5-10 sccm, substrate temperature between 300-600 ºC, deposition time 7-20 minutes, and radio-frequency power between 100-150 W. This research covers both experimental and simulation works including the classical theory of nucleation. Generally, important parameters were first calculated then simulated using computer programming, and finally matched in order to estimate the values of critical energy ΔG^*, critical radius r^*, surface energy γ, and free energy change per unit area ΔG_v. The associated Volmer-Weber growth mode was then predicted. Observably, optimum growth parameters for the inception of silicon nanodots were found to be at 600 ºC/10 minutes/100W formed on corning glass substrate. Structural and optical properties have been characterized using atomic force microscope AFM, energy-dispersive X-ray spectroscopy EDX, X-Ray diffraction XRD, photoluminescence PL and scanning electron microscopy SEM. In addition, the AFM characterization results show the existence of nanodots with the estimated average size of 34.4 nm. The results from PL spectrum reveal the presence of a peak which corresponds to a bandgap energy of 1.80 eV and this was attributed to the quantum confinement of electron–hole pairs in quantum wells. A further confirmation using EDX measurement was made which showed the existence of 0.48 at.% of silicon on the substrate. XRD analysis reveals the crystalline structure for high temperature conditions due to orderly silicon nanodots formed on the substrate. The results proved that the properties of silicon nanodots on quartz SiO_2, corning glass (7059) and silicon substrates were strongly dependent on the experimental conditions.

ABSTRAK

Bintik-nanosilikon merupakan satu bahan nano berdimensi sifar yang dikaji bagi kegunaan peranti elektron tunggal dalam litar bersepadu. Kajian ini cuba mendalami bahan yang semakin diminati di kenali sebagai bintik-nanosilikon yang terbentuk-sendiri pada substrat berbeza, dengan tumpuan kepada teori pertumbuhan dan penciriannya. Percanggahan mengenai teori pertumbuhan telah menyebabkan kecelaruan dan oleh itu pendekatan yang lebih inovasi dipersembahkan dalam kajian ini bagi meleraikan masalah sedia ada. Satu kaedah percikan frekuensi magnetron telah digunakan bagi menghasilkan bintik-nanosilikon pada keadaan berikut: kadar aliran gas argon 5-10 sccm, suhu substrat diantara 300-600 ºC, masa pemendapan 7-20 minit, dan kuasa frekuensi-radio 100-150 W. Penyelidikan ini merangkumi kedua-dua eksperimen dan kerja simulasi termasuk teori klasik mengenai penukleusan. Pada dasarnya, parameter yang penting dikira terlebih dahulu ke mudian di simulasi kan menggunakan program komputer dan akhirnya disepadankan kedua-duanya bagi memperolehi nilai-nilai tenaga genting ΔG^*, jejari genting r^*, tenaga permukan γ, dan perubahan tenaga bebas per unit luas ΔGv. Mod pertumbuhan Volmer-Weber kemudiannya boleh diramalkan daripada hasil tersebut. Secara pemerhatian di dapati bahawa parameter pertumbuhan yang optimum bagi bintik-nano silicon adalah 500 ºC/ 10 minit/ 100 W pada substrat kaca corning. Pencirian sifat-sifat struktur dan optik telah di lakukan dengan menggunakan mikroskop daya atom AFM, sinar-X sebaran elektron EDX, pembelauan sinar-X XRD, luminesenfoto PL dan mikroskop electron imbasan SEM. Sebagai tambahan, keputusan pencirian AFM telah menunjukkan tentang kewujudan bintik-nano dengan anggaran saiz sekitar 34.4 nm. Keputusan spectrum PL pula memaparkan adanya satu puncak dengan tenaga jalur jurang 1.80 eV yang boleh dikaitkan dengan pemerangkapan kuantum bagi pasangan electron-lohong dalam perigi kuantum. Seterusnya keputusan yang diperolehi telah di sahkan dengan menggunakan pengukuran EDX dimana sebanyak 0.48 atom.% kandungan silikon wujud pada permukaan substrat. Pemerhatian analisis XRD pula memperlihatkan struktur hablur bagi suhu tinggi yang disebabkan oleh pembentukan bintik-nanosilikon yang lebih teratur pada permukaan substrat, Semua keputusan di atas membuktikan bahawa sifat-sifat bintik-nanosilikon pada substrat SiO_2, kaca corning (7059) dan silikon adalah sangat bergantung kepada keadaan eksperimen.

TABLE OF CONTENTS

CHAPTER	TITLE	PAGE
	DECLARATION	ii
	DEDICATION	iii
	ACKNOLEDGEMENTS	iv
	ABSTRACT	v
	ABSTRAK	vi
	TABLE OF CONTENTS	vii
	LIST OF TABLES	xi
	LIST OF FIGURES	xii
	LIST OF ABBREVIATIONS	xvii
	LIST OF SYMBOLS	xix
	LIST OF APPENDICES	xxiii
1	**INTRODUCTION**	**1**
	1.1 Research Background	1
	1.2 Statement of Problem	5
	1.3 Research Objectives	9
	1.4 Scope of The Study	10
	1.5 Significance of The Study	11
2	**LITERATURE REVIEW**	**12**
	2.1 Introduction	12
	2.2 Bulk Material and Quantum Dots	12
	2.3 Structure Properties of Silicon Nanocrystals	14
	2.4 Optical Properties of Silicon Nanocrystals	15
	2.5 The Quantum Well and Multilayers	20

2.6 Classical Theory of Nucleation 26
2.6.1 Homogeneous Nucleation 28
2.6.2 Heterogeneous Nucleation: 33
2.7 The Growth Modes 35
2.8 Chemical Vapour Deposition (CVD) 39
2.9 Physical Vapour Deposition (PVD) 39
2.10 Radio Frequency Magnetron Sputtering 43
2.11 Sputtering Yield 47
2.12 Chapter summary 48

3 RESEARCH METHODOLOGY 49
3.1 Introduction 49
3.2 Simulation Program 49
3.3 Nanodots Growth Procedure 54
3.3.1 Sample Preparation 54
3.3.2 Quartz Substrate 55
3.3.3 Corning Glass (7059) Properties (Barium Borosilicate) 56
3.3.4 Silicon Substrate 56
3.4 Radio Frequency Magnetron Sputtering System 57
3.5 High Vacuum Coater Setting Parameters 62
3.5.1 Si/SiO_2 Thin Film Growth Parameters 62
3.5.2 Nanodots Growth Parameters 63
3.5.3 Rapid Thermal Annealing Parameters 67
3.6 QDs Measurements 68
3.6.1 Atomic Force Microscopy (AFM) 68
3.6.2 Photoluminescence (PL) 69
3.6.3 Energy Dispersive X-Ray Spectroscopy (EDX) 72
3.6.4 X-ray Diffraction (XRD) 73
3.6.5 Scanning Electron Microscope (SEM) 77
3.7 Chapter Summary 78

4	**RESULTS AND DISCUSSIONS**	**79**
	4.1 Introduction	79
	4.2 Simulation Result	80
	4.3 Surface Morphology Analysis	84
	4.4 Atomic Force Microscopy (AFM) Measurements	85
	4.4.1 Quartz Substrate	85
	4.4.2 Corning Glass Substrate	94
	4.4.3 Silicon Substrate	102
	4.4.4 Silicon Thin Film Annealing	108
	4.5 The Growth of Si/SiO_2 Thin Film	111
	4.6 Scanning Electron Microscopy (SEM) Measurement	112
	4.7 Energy Dispersive X-ray Spectroscopy (EDX) Measurement	114
	4.7.1 Quartz Substrate	114
	4.7.2 Corning Glass (7059) Substrate	116
	4.7.3 Silicon Substrate	118
	4.8 High Resolution X-ray Diffraction (HR-XRD)	120
	4.9 Photoluminescence (PL)	124
	4.9.1 Corning Glass (7059) Substrate	124
	4.9.2 Silicon Substrate	128
	4.9.3 Si/SiO_2 Thin Film	132
	4.10 Chapter Summary	138
5	**CONCLUSION**	**140**
	5.1 Summary	140
	5.2 Suggestions and Future Work	142
REFERENCES		143
Appendices A - B		153

LIST OF TABLES

TABLE NO	TITLE	PAGE
2.1	The four main dimensionality arrangements	18
3.1	The SiNDs growth parameters for quartz substrate at fixed RF power = 100 W.	62
3.2	The SiNDs growth parameters for corning glass (7059) substrate.	64
3.3	The SiNDs growth parameters for each SiO_2 substrate	65
3.4	SiNDs and Si/SiO_2 thin films annealing parameters under N_2 flow rate at fixed gas pressure 200 Pa.	66
3.5	Si thin films annealing parameters - N_2 gas pressure 200 Pa.	67
4.1	Experimental parameters and simulation result	80
4.2	Average dots size and surface roughness with deposition times.	88
4.3	Average dots size and surface roughness with substrate temperature.	90
4.4	Average dots size and surface roughness with substrate temperature.	100
4.5	Average dots size and surface roughness with deposition times.	101
4.6	Average dots size and surface roughness with substrate	106

	temperature.	
4.7	Average dots size and surface roughness with deposition times.	107
4.8	Annealing temperature with islands density.	110
4.9	Atomic and weight composition of silicon thin film deposition on quartz substrate at different deposition times.	115
4.10	Atomic and weight composition of silicon grown on corning glass (7059) substrate at different times of deposition.	117
4.11	Atomic and weight composition of silicon grown on silicon substrate at different deposition times.	119
4.12	Size of Si (100) nanocrystals as estimated from (400) Bragg diffraction for samples deposited at various deposition times.	123
4.13	Substrate annealing temperature and average grain size with the surface roughness.	137

LIST OF FIGURES

FIGURE NO	TITLE	PAGE
1.1	The crystalline and amorphous silicon thin film nanostructure.	6
	Silicon thin film deposition and the growth parameters of RF magnetron sputtering system.	7
1.3	The literature survey of radio frequency magnetron sputtering.	8
2.1	Meeting Bottom-up technique and top-down technique.	13
2.2	Electron-beam lithography processing for single-electron device fabrication.	14
2.3	Silicon four valance electrons.	15
2.4	Electron's orbit around the single nucleus.	16
2.5	Energy transition among VB and CB levels for: (a) bulk Si, (b) Quantum dots.	17
2.6	(a) Si indirect and (b) GaAs direct energy gap.	19
2.7	The diagram of optical transition of SiO_2/Si/SiO_2 multilayers as a quantum confinement in PL1 influenced by Si sublayer thickness and (b) Si/SiO_2 interface PL2.	20
2.8	PL spectrums obtained for MLs while only the Si sublayer thickness varies.	22
2.9	PL spectrums for Si/SiO_2 multilayers with varied Si layer thickness: (a) – (c) 4.5 nm, (d) 3 nm, (e) 1.5 nm, also (a) as-deposited, annealed at (b) 800 °C, and (c),(d),(e)1100 °C.	23
2.10	The XRD patterns of the Si/SiO_2 multilayers annealed at as-deposited 800–1100 °C.	23
2.11	The AFM images of the Ge/Si thin films growth at varied sputtering powers: (a) 2 W/cm^2; (b) 6 W/cm^2.	24
2.12	Normalized PL peaks for samples with SiNDs diameters from 1.8	25

	to 7 nm.	
2.13	PL spectrums for amorphous Si films grown at substrate temperature 200 °C and filament temperatures: 1 – 1735 °C, 2 – 1785 °C and 3 – 1881 °C.	25
2.14	The atomic nucleation and deposition process.	26
2.15	(a) Homogeneous nucleation, (b) heterogeneous nucleation.	27
2.16	Configuration of microcrystallites by liquid.	28
2.17	Nucleation of nanocrystallites. (a) Variation of Δg_a vs. temperature, $\Delta g_a = 0$ at T_d. (b) Variation of ΔG_f, free enthalpy of nucleus formation, vs radius of nucleus.	31
2.18	Quantum dot formation and three surface energies.	33
2.19	Three growth modes (F-M, V-W and S-K mode).	36
2.20	PVD and CVD vapor deposition.	39
2.21	RF magnetron sputtering system.	41
3.1	The simulation procedure flow chart.	49
3.2	Software program via heterogeneous nucleation.	50
3.3	Heterogeneous nucleation software toolbar (plot graphs display).	51
3.4	Heterogeneous nucleation software toolbar (Goto display).	51
3.5	Software program via homogeneous nucleation.	53
3.6	(a) The three substrates of Silicon, corning glass (7059) and quartz, (b) substrate holder with screw, (c) Purity of 99.99999% SiO_2 target, (d) Purity of 99.99999% Si target.	55
3.7	High Vacuum Chamber.	58
3.8	The substrate heater in HVC system.	59
3.9	Radio-frequency magnetron sputtering system.	60
3.10	Si/SiO_2 thin films deposition flow chart.	61
3.11	SiNDs and SiO_2 experimental procedure.	62
3.12	Schematic diagram AFM instrument.	8
3.13	Quantum well and quantum dot luminescence.	71
3.14	PL instrument structure.	72
3.15	(a) Emission of x-ray by an atom, (b) Elementary processes visualized in the term of scheme.	73
3.16	Crystal diffraction of X-ray.	74

3.17	X-ray diffraction of crystal solid and liquid or amorphous solid.	75
3.18	Diffraction of X-ray beam by crystal.	76
	SEM instrument structure.	77
4.1	(a) Simulation and (b) Experimental nanodots configuration result.	81
4.2	Critical energy versus temperature.	82
4.3	Critical radius versus temperature.	82
4.4	AFM topography image of blank Si wafer with RMS of 0.0532 nm.	80
4.5	AFM image for SiNDs grown on quartz substrate RF power 100 W, gas flow rate 5 Sccm and deposition times (a) 12, (b) 15 min temperature of 200 °C (scan area 1000 nm).	84
4.6	AFM image for SiNDs deposited on quartz substrate RF power 100 W, gas flow rate 5 Sccm, deposition time 15 mins, substrate temperature 200 °C with surface roughness 0.47 nm.	85
4.7	AFM image for SiNDs grown on quartz substrate RF power 100 W, gas flow rate 5 Sccm, deposition time 5 min temperature of 600 °C.	86
4.8	Average dots size and surface roughness versus substrate temperature.	87
4.9	AFM image for SiNDs grown on quartz substrate at different deposition times (a) 5, (b) 7, (c) 10, (d) 15 min, temperature of 200 °C, RF power 100 W and gas flow rate 5 Sccm.	88
4.10	Average dots size and surface roughness versus deposition time.	89
4.11	AFM image for SiNDs grown on quartz substrate at different deposition times (a) 5, (b) 7, (c) 10, (d) 15 min, temperature of 200 °C, RF power 100 W and gas flow rate 10 Sccm.	90
4.12	AFM image for SiNDs grown on quartz substrate at different deposition times (a) 5, (b) 7, (c) 10, (d) 15 min, temperature of 300 °C, RF power 100 W and gas flow rate 10 Sccm.	92
4.13	AFM image for SiNDs grown on quartz substrate at different deposition times (a) 5, (b) 7, (c) 10, (d) 15 min, temperature of 300 °C, RF power 100 W and gas flow rate 5 Sccm.	93
4.14	AFM dot size measurement for SiNDs grown on corning glass	94

substrate at deposition time of 10 min, temperature of 600 °C, RF power 100 W and gas flow rate 5 Sccm.

4.15 AFM image for SiNDs grown on corning glass substrate at different deposition times (a) 5, (b) 7, (c) 10, (d) 15 min, temperature of 600 °C, RF power 150 W and gas flow rate 5 Sccm at scan area 1000 nm. 95

4.16 AFM image for SiNDs grown on corning glass (7059) substrate at different deposition times (a) 5, (b) 7, (c) 10, (d) 15 min, temperature of 500 °C, RF power 100 W and gas flow rate 5 Sccm. 96

4.17 AFM image for SiNDs grown on corning glass (7059) substrate at different deposition times (a) 5, (b) 7, (c) 10, (d) 15 min, temperature of 400 °C, RF power 100 W and gas flow rate 5 Sccm. 97

4.18 AFM image for SiNDs grown on corning glass (7059) substrate at different deposition times (a) 5, (b) 7, (c) 10, (d) 15 min, temperature of 400 °C, RF power 150 W and gas flow rate 5 Sccm. 98

4.19 AFM image for SiNDs grown on corning glass substrate at different deposition times (a) 5, (b) 7, (c) 10, (d) 15 min, temperature of 400 °C, RF power 150 W and gas flow rate 10 Sccm. 99

4.20 Average dots size and surface roughness versus the Substrate temperature. 100

4.21 Average dots size and surface roughness versus the deposition times. 101

4.22 AFM (a) 3D Images (b) cross section for SiNDs grown at temperature 600 °C, RF power 100 W and deposition time 10 min, at scan area 500 nm. 102

4.23 AFM images of SiNDs grown on silicon substrate at different deposition times (a) 5, (b) 7, (c) 10, (d) 15 min, temperature of 400 °C, RF power 100 W and gas flow rate 5 Sccm. 103

4.24 AFM image for SiNDs grown on silicon substrate at different 103

	deposition times (a) 5, (b) 7, (c) 10, (d) 15 min, temperature of 500 °C, RF power 150 W and gas flow rate 5 Sccm.	
4.25	AFM images of SiNDs grown on silicon substrate at different deposition times (a) 5, (b) 7, (c) 10, (d) 15 min, temperature of 500 °C, RF power 100 W and gas flow rate 5 Sccm.	105
4.26	AFM images for SiNDs deposited on silicon substrate at 15 mins deposition time, substrate temperature 500 °C, RF power 150 W and gas flow rate 5 Sccm.	105
4.27	Average dots size and the surface roughness with substrate temperature.	106
4.28	Average dots size and the surface roughness with substrate deposition times.	107
4.29	AFM images of silicon NDs grown on silicon substrate: (a) before annealing (5000 nm scan area), (b) before annealing (1000 nm scan area), (c) after annealing for 5 min and 600 °C (5000 nm scan area), (d) after annealing for 5 min and 600 °C (1000 nm scan area) (e) after annealing for 10 min and 800 °C (5000 nm scan area), (f) after annealing for 10 min and 800 °C (1000 nm scan area).	109
4.30	AFM images of Si/SiO_2 grown on silicon substrate at different deposition times (a) as-SiO_2 deposited, (b) 5, (c) 10, (d) 15 min for Si, temperature of 400 °C, RF power 100 W and gas flow rate 5 Sccm.	110
4.31	Plan-view SEM image for Si/SiO_2 multilayers grown on silicon substrate: (a) Si nanoparticles view and (b) Si nanoparticles size measurement at time of deposition 10 min temperature of 400 °C, RF power 100 W and gas flow rate 10 Sccm.	112
4.32	Cross-section view SEM for Si/$_{SiO2}$ multilayers grown on silicon substrate at different deposition time 10 min (a) Si and (b)Si/SiO_2 thin films thickness, temperature of 400 °C, RF power 100 W and gas flow rate 10 Sccm.	113
4.33	EDX patterns of quartz substrate before silicon thin film deposition.	114

4.34	EDX patterns of silicon nanodots growth on quartz substrate with deposition time 10 min, substrate temperature 400 °C, and RF power 100 W.	115
4.35	EDX patterns of corning glass substrate before silicon nanodots deposition.	116
4.36	EDX patterns of Silicon nanodots growth on corning glass (7059) substrate with deposition time 10 min, substrate temperature 400 °C and RF power 100 W.	117
4.37	EDX pattern of silicon substrate before silicon nanodots deposition.	118
4.38	EDX patterns of silicon nanodots growth on silicon substrate with deposition time 10 min, substrate temperature 400 °C, and RF power 100 W.	119
4.39	XRD patterns of bulk crystalline Si.	120
4.40	XRD patterns of silicon substrate.	121
4.41	XRD patterns of SiNDs growth on silicon substrate at different deposition times: (a) before deposition, (b) 8, (c) 10, (d) 15 min and substrate temperature 450 °C, RF power 100 W, and gas flow rate 5 sccm.	122
4.42	Photoluminescence characterization for SiNDs grown on corning glass at time of deposition 5 min, RF power 100 W and different temperature (a) 300, (b) 400, (c) 500, (d) 600 °C.	125
4.43	Photoluminescence characterization for SiNDs grown on corning glass at time of deposition 15 min, RF power 100 W and different temperature (a) 300, (b) 400, (c) 500, (d) 600 °C.	126
4.44	Photoluminescence characterization for SiNDs grown on corning glass at growth temperature 500 °C, RF power 100 W and different deposition times (a) 5, (b) 7, (c) 10, (d) 15 min	127
4.45	Photoluminescence characterization for SiNDs grown on silicon at growth temperature 500 °C, RF power 100 W and different deposition times (a) 5, (b) 7, (c) 10, (d) 15 min.	129
4.46	Photoluminescence characterization of SiNDs grown on silicon at growth temperature 400 °C, RF power 100 W and different	129

deposition times (a) 7, (b) 10, (c) 15, (d) 20 min.

4.47 Photoluminescence characterization for SiNDs grown on silicon at time of deposition 15 min, RF power 100 W and different temperature (a) 300, (b) 400, (c) 450, (d) 500 °C. 130

4.48 Photoluminescence characterization for SiNDs grown at silicon substrate and annealing at different temperature (a) as-deposit, (b) 500, (c) 600, (d) 700, (e) 800 °C. 131

4.49 Photoluminescence characterization for Si/SiO_2 thin film grown on silicon at growth temperature 500 °C, RF power 100 W and different deposition times (a) 5, (b) 7, (c) 10, (d) 15 min. 133

4.50 Photoluminescence characterization for Si/SiO_2 thin film grown on silicon at growth temperature 600 °C, RF power 100 W and different deposition times (a) 5, (b) 7, (c) 10, (d) 15 min. 134

4.51 Photoluminescence characterization for Si/SiO_2 thin film grown on silicon at time of deposition 15 min, RF power 100 W and different temperature (a) 300, (b) 400, (c) 500, (d) 600 °C. 135

4.52 Photoluminescence characterization for Si/SiO_2 thin film annealing at different temperature (a) as-deposit, (b) 500, (c) 600, (d) 700, (e) 800 °C. 136

4.53 Annealing temperature versus the energy gap for both Si and Si/SiO_2 samples. 137

LIST OF ABBREVIATIONS

AFM	-	Atomic force microscope
AO	-	Atomic orbit
CB	-	Conduction band
CVD	-	Chemical vapor deposition
DC	-	Direct current
EBL	-	Electron beam lithography
EDX	-	Energy dispersive X-ray
FESEM	-	Field emission scanning electron microscope
F-M	-	Frank Vander Merwe
FWHM	-	Full width at half maximum
HRTEM	-	High resolution transmission electron microscope
HVC	-	High vacuum coater
ITRS	-	International technology roadmap of semiconductor
LC	-	Loading circuit
LCD	-	Liquid crystal display
LPCVD	-	Low pressure chemical vapor deposition
MBE	-	Molecular beam epitaxy
ML	-	Multilayer
Mo	-	Molecular orbit
MosFETs	-	Metal oxide semiconductor field effect transistor
A_n	-	Nanoparticles
Nb_3Ge	-	Niobium germanium
n	-	Number of atoms
0D	-	One dimension

PL	-	Photoluminescence
PECVD	-	Plasma-enhanced chemical vapour deposition
PL	-	Photoluminescence
Ps	-	Porous silicon
PVD	-	Physical vapour deposition
QC	-	Quantum confinement
QW	-	Quantum well
RF	-	Radio frequency
RIE	-	Reactive ion etching
RMS	-	Root mean square
RTP	-	Rapid thermal annealing processing
S,P,D,F	-	Spherical orbit
SEM	-	Scanning electron microscope
SiNDs	-	Silicon nanodot
SiQDs	-	Silicon quantum dots
S-K	-	Stranski Krastanov
SiNWs	-	Silicon nanowire
TRE	-	Thermally reactive evaporation
3D	-	Three dimensions
TEM	-	Transmission electron microscope
2D	-	Two dimensions
UHV	-	Ultra high vacuum
VB	-	Valence band
VLSI	-	Very large scale integrated circuits
V-W	-	Volmer Weber
GIXRD	-	Grazing incidence X-ray diffraction
0D	-	Zero dimension
	-	Extreme programming

LIST OF SYMBOLS

a	-	New phase volume
Ar	-	Argon
Ar^{+}	-	Argon ion
a-Si	-	Amorphous silicon
at. %	-	Atomic percentage
c	-	Radius of nuclei
c^{*}_{hetro}	-	Critical radius for heterogeneous
c^{*}_{homo}	-	Critical radius for homogenous
c_i	-	Number of nuclei atoms
c_0	-	Number of liquid atoms
c-Si	-	Crystalline silicon
e^{-}	-	Electron
E_c	-	Conduction energy
E_g	-	Energy bandgap
Ek	-	The kinetic energy
eV	-	Electron Volt
Ga	-	Gallium
As	-	Arsenide
Ge	-	Germanium
$h, \hbar$	-	Planck’s constant
K	-	Boltzmann constant
k	-	Wavevector or momentum vector
L_h	-	Latent heat of the material fusion per unit of volume
m	-	Effective mass

N	-	Dimensionality
N_c	-	Directions of confinement
N_f	-	Freedom grades
N_2	-	Nitrogen
O	-	Oxygen
RMS	-	Root mean square roughness
Si	-	Silicon
SiO	-	Silicon monoxide
SiO_2	-	Silicon dioxide
Si-O	-	Silicon oxide bond
sccm	-	Standard cubic centimeters per minute
T	-	Temperature
T_d	-	Transition temperature or solidification temperature
2Θ	-	Diffraction angle (two-theta)
$<$	-	Less than
γ	-	Surface energy change per unit area
γ_S	-	Surface energy between the liquid-substrate
γ_N	-	Surface energy between the liquid-solid nucleus
γ_{NS}	-	Surface energy between the solid nucleus-substrate
ΔC_v	-	Variation in specific heat
ΔC^h_v	-	Variation in the specific heats at the melting point
ΔE	-	Energy gap
ΔG	-	The total variation in free energy
ΔG_a	-	Variation in free energy change per unit volume
ΔG_c	-	Variation in free energy change per unit surface
Δg_a	-	Free enthalpy per unit volume
ΔG_f	-	Net change of energy for homogenous nucleation
ΔG^*_f	-	Critical energy for homogenous nucleation
Δh_a	-	Change in enthalpy
Δs_a	-	Entropy change

ΔT	-	Undercooling temperature
θ	-	Contact Angle
λ	-	Wavelength
π	-	Pi = 3.1415926
v_o	-	Molecular volume
v	-	Velocity

LIST OF APPENDICES

APPENDIX	TITLE	PAGE
A	Photographs of Experimental Equipments	153
B	Published Papers	156

CHAPTER 1

INTRODUCTION

1.1 Research Background

From the beginning of the last century, nanotechnology has become one of the most common techniques promising for new artificial atoms having diameter less than 100 nm to fabricate nanodevices into single integrated chip [1,2]. Now the International Technology Roadmap of Semiconductors (ITRS) predicts that the physical gate length of high performance metal oxide semiconductor field effect transistor (MOSFETs) will reach sub 10 nm in 2016 [3]. Therefore, the fast improvement in the fabrication techniques of silicon electronic devices and single electron very large scale integrated circuits (VLSI) has been achieved. This has been gradually developed by miniaturizing the device dimensions by exponential growth of microelectronics capabilities. Currently, single electron transistor device was reported using silicon self-assembled nanodots (NDs) and room temperature characteristics have been measured. Consequently, there is a chance for using SiNDs as a memory cell, due to the nanodots parallel to the multitunnel junction structure that has strong changed of random background charges. On the other hand, maintaining the conventional top-down methods improvement becomes very hard due to the basic phenomena, scientific confines and cost effectiveness [4].

Thin film semiconductors devices around over decades have been fabricated by a thin film deposited on a semiconductor substrate. However the integrated

electronic circuits system depends on electrical charges confined in the interfaces between different materials with different electronic properties. This system created by composite different materials of the thin film such as thin films deposition that has the desired properties on substrate. The material structure applications at high temperature depend on thin film methods to provide the suitable coating, increase the efficiency and increase the material lifetime. The surface and near surface properties are important in varying the functionality of the material (catalysis, deformation, electrical and optical properties). Hence, rapidly growing of economics and application require high performance, low cost, compact and reliable adaptable devices that are driving the technology of thin film.

The fabrication of thin film microstructure must carry out the influences of contaminations in the vapour phase, kinetic energy of the incident ions, base pressure, deposition rate, nature of substrate material, substrate temperature; in addition, its surface cleanliness, nanostructure. The deposited microstructure can also be affected by energetic particles such as electron photon and ion bombardment. Operating the growth parameters permits to avoid the defects in the depositing polycrystalline film, as well as control the point of thin film thickness and grain size in thin films, which is only possible in some cases with certain deposition process. In integrated circuits a low resistivity film and high threshold current density is required for interconnections by semiconducting films. All of these properties are particularly influenced by the fault structure of the film, and in fact it depends on the techniques used to fabricate the thin film [5].

The technique of thin film deposition has four stages. First, the essential configuration of the vapor phase from the condensed phase and its properties. There are some methods of vapor formation such as evaporation, sputtering, electron beam evaporation and ion deposition. The second stage is the transport of ionized particles from the target to the substrate. Also some techniques consider the reactivation of evaporated atoms during the transport to the substrate such as reactive evaporation, electron cyclotron resonance plasma assisted growth and other else. The most important field of thin film fabrication is the study of the capability to form an epitaxial thin film. This capability has exclusive control the formation, construction

and faults of the thin film. Thirdly, concerning those procedures that lead to reorganize the coalescence on the substrate surface, or rearrange the structure of the thin film to give the desired properties for the device. Some characteristics are desired to fabricate the final microstructure of the thin film appearance indicates the controlling of nanostructure and surface morphology of the thin films by set the defects position as preferred or give them the desired crystal structure [5,6].

Self-assembled Si nanostructure deposition by using radio frequency sputtering technique has much recommended for large-scale integrated circuits fabrication. The production of silicon nanostructures has opportunity to use for electrical devices. The magnetron sputtering method becomes one of the most common methods for fabricating the silicon nanostructures due to high deposition rate and safety currently [2]. In fact to make sufficient devices, it is important to improve the methods which permit the commercial production of semiconductor thin films. The usual ions transportation from target to substrate will establish the regularity of that thin film. The real properties of the film are affected by the substrate selected and its surface cleanliness. Moreover the nanostructure of the films through deposition depends on different parameters, such as the substrate temperature, ion energy and angle of incidence of the depositing particles [7].

Thin film techniques are important to produce nanoscale materials, such as quantum wires, quantum dots and superlattices. All these structures make thin film field not only more attractive material properties and process reliant, but also give interesting novels to explain the material phenomena. Thin film properties are clearly related to the existence of surface at two materials in close connection with each other. Where the properties vary from bulk material, divides the amount of atoms at any time on the surface on average 10^{10} atoms/m [5].

Nanostructure of materials and its properties (the electron and phonon states) change radically as their size decrease in one or more dimensions to nanometer scale, that have follow down almost the atomic energy levels [8]. Si nanodots are one of typical materials used in nanotechnologies, because of their unique and useful

functions originating from quantized electron energy state [3]. The observed visible luminescence at room temperature from Si gives attention to improve the electronic and oscillation properties of silicon nanocrystals. The recognized electronic devices motivates many investigations of different Si nanostructures using varied preparation methods. Currently, research in nanocrystalline silicon nc-Si confirmed considerable changes in the luminescence properties and energy levels, due to quantum confinement caused by the miniaturized size of the particles and a collapse of *k*-vector protection [9]. In addition, zero- and one dimensional nature of electronic states in the individual SiNDs realizes new electronic and photonic properties, which are not achieved with bulk silicon [3]. Nevertheless, the observations show some disagreement with QC create from other phenomenon that may come from the PL. However, the PL properties are clearly following the measured structure (composite, ML, amorphous, crystalline, etc.) and also depend on the fabrication method [2].

In the practical applications, it is important to form high-density and similarly-sized SiNDs. Although various formation techniques have been developed so far, it is generally difficult to achieve high-density and nanometer-size with low dispersion of distribution simultaneously. Silicon nanostructures can be formed on non-Si substrates, such as glass and plastic, the Si-based bottom-up approach may lead to high performance and large-area electronics [8].

The research area of nanostructure silicon fabrication methods have been widely improved last time as the finding of room-temperature photoluminescence PL function of porous silicon. The researchers were faithful to nanodots structures 0D and to layered formations 2D for the construction of optoelectronic devices suitable for the silicon structure, due to the strong mechanical performance and stable porous silicon 1D. For explaining the combined materials consist of SiNDs embedded in apparent and insulating matrix SiO_2, they are usually prepared using plasma enhanced chemical vapour deposition PECVD or by magnetron sputtering of Si^+ ion implantation in thermally grown silica. The ML structure clears more fitting than the complex material, while it presents at least a confident of the nanoparticles size in the formation method [2, 10]. Moreover, hard and costly equipment of molecular beam epitaxy system which limits the number of multilayers. On the other hand, the

magnetron sputtering technique shows more improving of visible photoluminescence Si/SiO_2 [11].

The accurately controlled nanostructures can be fabricated easily using self-assembly of atoms by operating the organic molecules as a structure block for nanoscale devices which have more consideration. This bottom-up approach changed the hard processes of the existing silicon top-down approach. Since the conductivity of the organic molecular configurations is less than silicon conductivity, the electron moving among the single molecule is mainly controlled by passing the conduction. Silicon nanodots SiNDs and nanowires SiNWs can give a resolution to these problems by assembling the involvements of both bottom-up approach and optimum electron transport. Since silicon nanostructures can be grown on non-Si substrates, such as glass and plastic, the silicon supported bottom-up techniques may guide to fine properties and wide electronics applications. However, nanostructure considers new electrical and photonic behaviors, which are not realized with bulk silicon. Also interconnecting the bottom-up approach with the classic top-down Si methods permit to investigate silicon nanoelectronics [5, 12].

1.2 Statement of Problem

Silicon nanostructure has two types: crystalline nanostructure which has regular periodic arrangement of atoms in the lattice structure such as Poly crystalline silicon, and amorphous that has dangling bonds and random arrangement of atoms such as hydrogenated amorphous silicon as shows in Fig 1.1. This nanostructure depends on the substrate temperature during thin film deposition. Therefore, high substrate temperature causes the kinetic energy of atoms exceeding the surface barrier and relocated during deposition; as a result, increase the surface roughness of the thin film. Whereas, low temperature causes the sputtered atoms lose their kinetic energy before catch the substrate and creates amorphous thin film nanostructure [13,14].

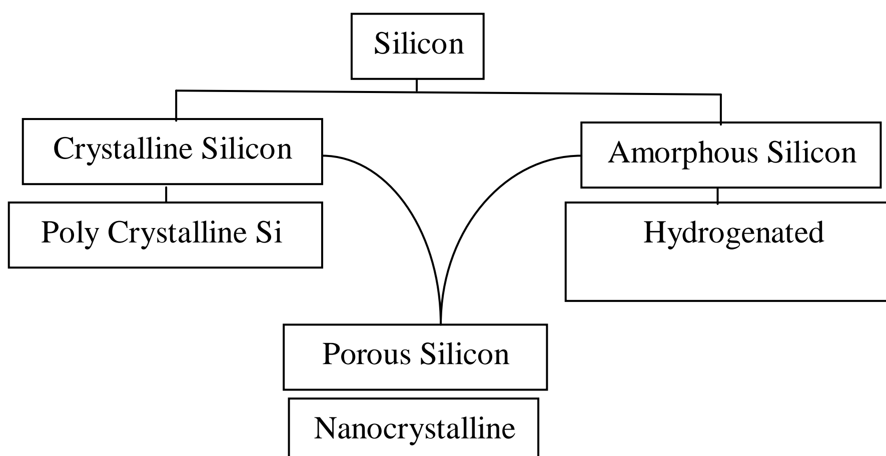

Figure 1.1 The crystalline and amorphous silicon thin film nanostructure.

Silicon nanofabrication is essential to motivate nanotechnology [15]. The real challenges in nanomaterials fabrication are the accuracy of the diameter and fine identified shapes. To fabricate a nanodevice, considerations must be given to nanoscale diameters, shapes, and properties of materials or components [16]. The silicon thin film nanostructure grown by using RF-magnetron sputtering system is affected by the different growth parameters such as substrate temperature as shows in Fig 1.2. However by changing the substrate temperature different nanodots diameter, islands density, islands shape, surface roughness, crystalline structure and optical properties could be obtained. It is essential to precise the size of the nanoparticles, their density, and surface morphology, as the emission in visible scope is clearly showed by a quantum confinement. Widely, the fabrication system applied these values and the reduction of nanodots size follow by energy gap increasing [17,18].

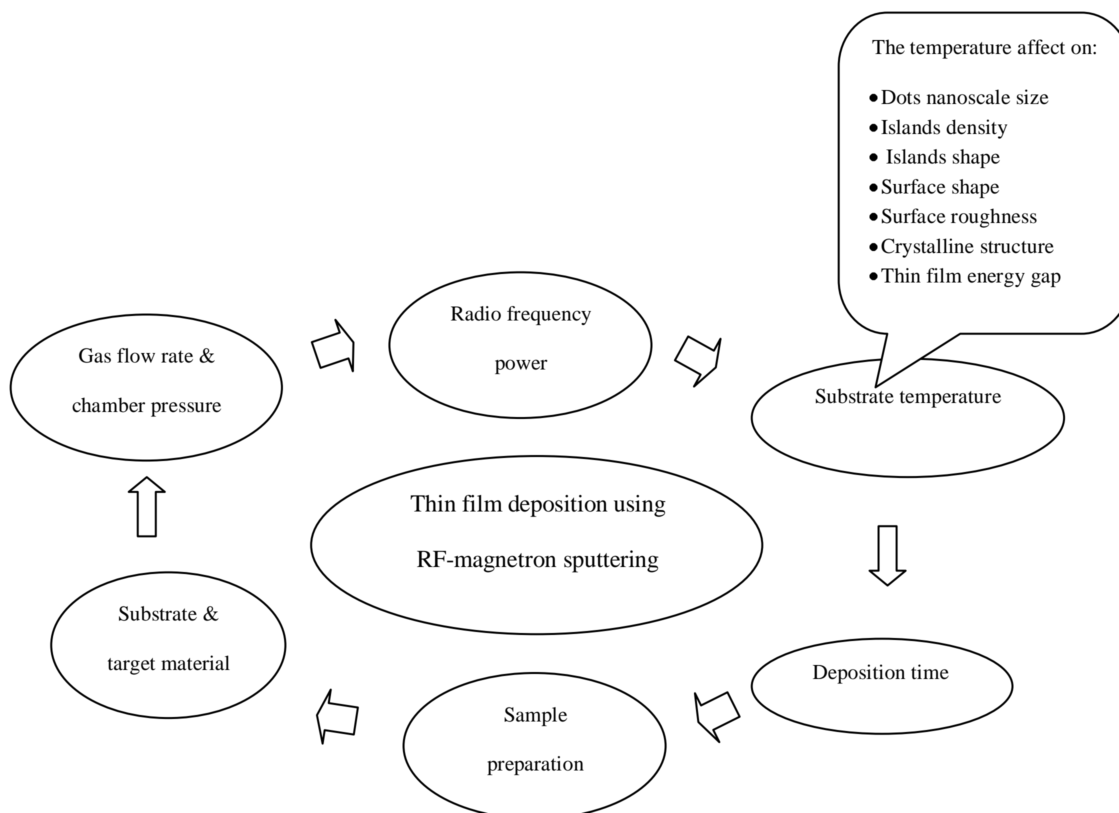

Figure 1.2 Silicon thin film deposition and the growth parameters of RF magnetron sputtering system.

There were few improvement of works using the conventional deposition techniques which discovered the formation of SiNDs with less identify structures. RF-magnetron sputtering system – which located at Ibnu Sina institute for fundamental studies, UTM - had been used [20,21] to deposit silicon thin films at substrate temperature less than 400 ˚C, as shows in Figure 1.3. Whereas low substrate temperature less than 300 ˚C cause defects (dangling bonds) in the thin film nanostructure, that create the random arrangement of the atoms in the lattice structure (amorphous structure).

In fact the silicon/silicon dioxide nanocrystal is desired for high electron mobility in the microelectronic devices, which is low in amorphous silicon. Therefore, by replacing each atom of silicon with oxygen [19] to reduce the typical defect like silicon dangling bonds, Si/SiO_2 multilayers could keep a lattice match for low defects [11, 17, 20-24].

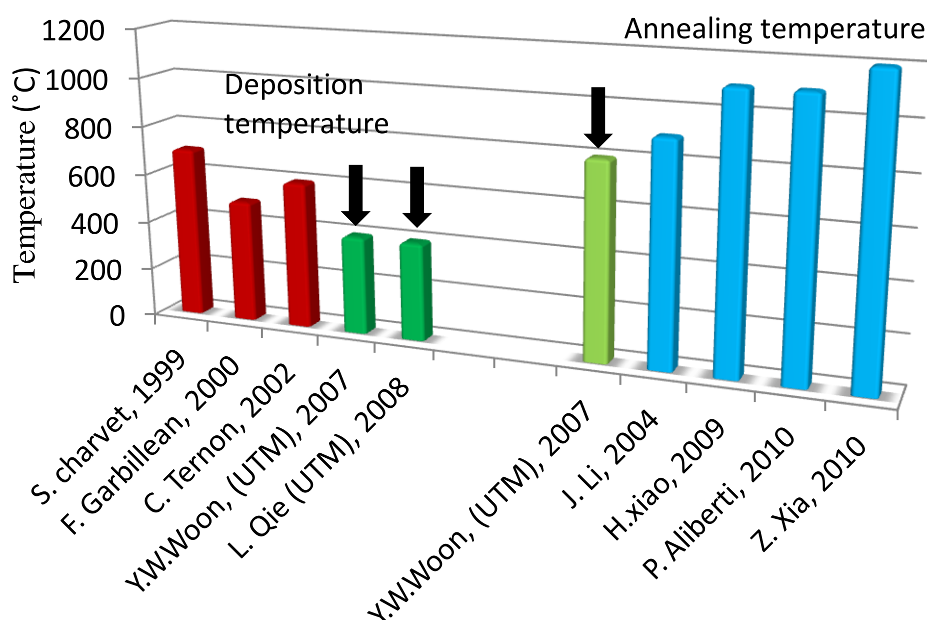

Figure 1.3 The literature survey of radio frequency magnetron sputtering.

This study is involved which will result in quality of the SiNDs fabrication on different substrates. The effect of temperature, chamber pressure, gas flow rate, and RF-power on structural, optical and electrical properties of SiNDs growth has been given attention so far. SiNDs deposited in plasma excitation radio frequency also depend on these parameters. So by varying these parameters, the corresponding structural and optical properties are expected to be significantly improved [7]. Therefore, to obtain silicon thin film with a high crystalline structure and high surface roughness, it is proposed to increase the substrate temperature until 500 ˚C or more.

Nucleation is a random process; in which the number of nuclei formed in a fixed period of times is a random quantity and is subject to statistical laws. However, the average values can be calculated and are subject to the kinetic theory of nucleation. This research has been done to compare the simulation results with the experimental works and confirm the classical theory of nucleation and growth mode of *Volmer- Weber*. The formation of SiNDs can be predicted using a simple model of the islands growth, where the atoms or vapours diffuse to each other

followed by agglomeration that form the nuclei of new phase. Thus, this research describes the nucleation and growth of silicon nanodots for the vapour/liquid transition with detailed analysis of parameters deduced from the theory and experimental [25].

1.3 Research Objectives

The objectives of this research as to:

1. Reestablish the simulation works in order to confirm the classical theory of nucleation and growth mode of *Volmer- Weber*.
2. Determine the optimum growth parameters of SiNDs and Si/SiO_2 interface for HVC system (deposition time, substrate temperature, gas flow rate, gas pressure, and radio frequency power), as well as modify the HVC system.
3. Characterize silicon thin film structural properties of surface roughness and nanndots size using AFM measurements follow by SEM measurement, and determine the silicon atomic percentage that has deposit on the substrate by used EDX measurements.
4. Characterize the energy gap (optical properties) of silicon thin film using PL measurement to confirm the reduction of nanodots size follow by energy gap increasing.
5. Characterize the grain (nanocrystal) size and silicon thin film crystalline structure using XRD measurements.

1.4 Scope of the Study

This research explains the theoretical and simulation procedure of heterogeneous nucleation. The simulation work represents the nucleation and growth theory, including the transition from liquid-solid phase, also to prove the appearance changing for net energy and nuclei size. The simulation program is conducted using Microsoft Visual Basic 6.0 professional. As well as to determine the calculated parameters using a computer programe are designed for a dome-like nucleus assumed in Volmer-Weber growth theory.

Recently self-assembly technique to fabricate SiNDs is experimentally carrying out by using radio frequency magnetron sputtering system for future nanodevice applications. In this research, the quartz SiO_2, corning glass (7059), and silicon wafer have been chosen as substrates. Therefore, the experimental conditions are identified at high substrate temperature of 600 ˚C in order to create silicon thin film with high crystalline structure. Consequently, this deposition process is performed using different growth parameters (deposition time, substrate temperature, gas flow rate, gas pressure, and radio frequency power). SiNDs structural properties are measured using AFM, EDX, SEM and XRD equipments following by optical properties using PL measurement to calculate the energy gap of silicon thin film.

1.5 Significance of the Study

This study is essential to enhance the understanding of SiNDs growth mechanism and its properties. The possibility to form a semiconductor thin film on the surface of the glass substrates open a new aspect in understanding the structure, electrical and optical properties of thin films. However these properties are attracting researchers to fabricate various structural properties which are absolutely unlike the naturally accessible properties [5].

Thin film deposition technique is adding new commercial devices and allowing further characteristic in fabrication. Therefore it is a promising to improve the devices utility and also keep the possessions materials wastes by the conventional fabrication methods. In addition the quantum confinement of charge carriers improves the field of nanostructure as influences the properties of materials. The key to convergence the computing, communications and consumer electronics is the optical, magnetic and electronic properties of thin films. It is apparent that thin film has an important function to influence humanity in the future [5].

Recently, research related to Si nanostructure has been given consideration and continuing trend towards integration of microelectronics and optoelectronics devices. However, bulk Si has an indirect band-gap structure that limited its application in optoelectronics for a very long time, due to the lower luminescence efficiency [27]. Silicon becomes the preferred material for single-electron and quantum electronic devices due to its unique structure, electrical and optical properties. Recently SiNDs applications in electronics device is recommended and agreed by the design of single memory and other devices requires the coulomb blockade effect [16].

REFRENCES

1. Bryant, G.W. and G. Solomon, *Optics of quantum dots and wires*. 2005: Artech House.
2. Ternon, F. Gourbilleau, R. Rizk, and C. Dufour, *Si/SiO$_2$ multilayers: synthesis by reactive magnetron sputtering and photoluminescence emission.* Physica E: Low-dimensional Systems and Nanostructures, 2003. **16**(3-4): p. 517-522.
3. Mizuta, H. and S. Oda, *Bottom-up approach to silicon nanoelectronics.* Microelectronics Journal, 2008. **39**(2): p. 171-176.
4. Zahi, H. Vergnes, B. Caussat, A. Estève, M. Djafari Rouhani, P. Mur, P. Blaise, and E. Scheid, *Towards multiscale modeling of Si nanocrystals LPCVD deposition on SiO$_2$: From ab initio calculations to reactor scale simulations.* Surface and Coatings Technology, 2007. **201**(22-23): p. 8854-8858.
5. SreeHarsha, *Principles of physical vapor deposition of thin films*. 2006: Elsevier.
6. Cha, G. Kim, H.J. Doerr, and R.F. Bunshah, *Effects of activated reactive evaporation process parameters on the microhardness of polycrystalline silicon carbide thin films.* Thin Solid Films, 1994. **253**(1-2): p. 212-217.
7. Yoo, C.S., *Semiconductor manufacturing technology*. 2008: World Scientific.
8. Henini, A. Patanè, A. Polimeni, A. Levin, L. Eaves, P.C. Main, and G. Hill, *Electrical and optical properties of self-assembled quantum dots.* Microelectronics Journal, 2002. **33**(4): p. 313-318.
9. Sirenko, R. Fox, I.A. Akimov, X. Xi, S. Ruvimov, and Z. Liliental-Weber, *In situ Raman scattering studies of the amorphous and crystalline Si nanoparticles.* Solid State Communications, 2000. **113**(10): p. 553-558.

10. Baron, T., F. Martin, P. Mur, C. Wyon, and M. Dupuy, *Silicon quantum dot nucleation on* Si_3N_4*,* SiO_2 *and* SiO_xN_y *substrates for nanoelectronic devices.* Journal of Crystal Growth, 2000. **209**(4): p. 1004-1008.
11. Gourbilleau, P. Voivenel, X. Portier, and R. Rizk, *A novel method for the deposition of Si-*SiO_2 *superlattices.* Microelectronics Reliability, 2000. **40**(4-5): p. 889-892.
12. Sun, and H.C. Kang, *Synthesis and characterization of self-assembled ZnO nano-dots grown on* SiN_x*/Si(001) substrates by radio frequency magnetron sputtering.* Thin Solid Films, 2010. **518**(22): p. 6522-6525.
13. S. Sakrani, F.A. Idrees, Z. Othaman, and A.K. Ismail, *The Growth Mechanism of Silicon Nanodots Synthesized by Sputtering Method.* AIP Conference Proceedings, 2011. **1341**(1): p. 109-113.
14. Lopez Villanueva, J.A. Jimenez Tejada, A. Palma, S. Rodriguez Bolivar, and J.E. Carceller. *A simple model to analyze electron confinement and trapping in silicon nanodots*. in *Electron Devices, 2005 Spanish Conference on*. 2005.
15. Teo, X.H. Sun, *Silicon-Based Low-Dimensional Nanomaterials and Nanodevices.* Chemical Reviews, 2007. **107**(5): p. 1454-1532.
16. Xiao, S. Huang, J. Zheng, G. Xie, and Y. Xie, *Optical characteristics of Si/*SiO_2 *multilayers prepared by magnetron sputtering.* Microelectronic Engineering, 2009. **86**(11): p. 2342-2346.
17. Huang, Z. Xia, H. Xiao, J. Zheng, Y. Xie, and G. Xie, *Structure and property of Ge/Si nanomultilayers prepared by magnetron sputtering.* Surface and Coatings Technology, 2009. **204**(5): p. 558-562.
18. Jung, Y.M. Jung, L.R. Shaginyan, and J.G. Han, *Polycrystalline Si thin film growth on glass using pulsed d.c. magnetron sputtering.* Thin Solid Films, 2002. **420-421**: p. 429-432.
19. Lewis, B. and J.C. Anderson, *Nucleation and growth of thin films*. 1978: Academic Press.
20. L.Qie Jie, 2008, *Silicon self-assembled nanodots prepared using radio frequency magnetron sputtering*, Master Thesis,Universiti Teknologi Malasyia, Skudai.
21. Yeong Wai Woon, 2007, *The formation structural and optical properties of silicon nanocrystals embedded in silicon dioxide*, Master Thesis, Universiti Teknologi Malaysia, Skudai.

22. Charvet, R. Madelon, F. Gourbilleau, and R. Rizk, *Ellipsometric spectroscopy study of photoluminescent Si/SiO_2 systems obtained by magnetron co-sputtering*. Journal of Luminescence, 1998. **80**(1-4): p. 257-261.
23. Ternon, F. Gourbilleau, X. Portier, P. Voivenel, and C. Dufour, *An original approach for the fabrication of Si/SiO_2 multilayers using reactive magnetron sputtering*. Thin Solid Films, 2002. **419**(1-2): p. 5-10.
24. Li, X.L. Wu, D.S. Hu, Y.M. Yang, T. Qiu, and J.C. Shen, *Splitting of X-ray diffraction peak in (Ge:SiO_2)/SiO_2 multilayers*. Solid State Communications, 2004. **131**(1): p. 21-25.
25. Aliberti, S.K. Shrestha, R. Teuscher, B. Zhang, M.A. Green, and G.J. Conibeer, *Study of silicon quantum dots in a SiO_2 matrix for energy selective contacts applications*. Solar Energy Materials and Solar Cells, 2010. **94**(11): p. 1936-1941.
26. Xia, Z. and S. Huang, *Structural and photoluminescence properties of silicon nanocrystals embedded in SiC matrix prepared by magnetron sputtering*. Solid State Communications, 2010. **150**(19-20): p. 914-918.
27. Kondo, T. Ueyama, E. Ikenaga, K. Kobayashi, A. Sakai, M. Ogawa, and S. Zaima, *Formation of high-density Si nanodots by agglomeration of ultra-thin amorphous Si films*. Thin Solid Films, 2008. **517**(1): p. 297-299.
28. Ruzmetov, Y. Seo, L.J. Belenky, D.M. Kim, X. Ke, H. Sun, V. Chandrasekhar, C.B. Eom, M.S. Rzchowski, and X. Pan, *Epitaxial magnetic perovskite nanostructures*. Advanced Materials, 2005. **17**(23): p. 2869-2872.
29. Ignac Capek, Slovak Academy of Sciences, Dúbravská cesta 9, Bratislava, Slovakia, *Chapter 1 Nanotechnology and nanomaterials*, in *Studies in Interface Science*, I. Capek, Editor. 2006, Elsevier. p. 1-69.
30. Diener, D. Kovalev, G. Polisski, and F. Koch, *Luminescence properties of two-photon excited silicon nanocrystals*. Optical Materials, 2001. **17**(1-2): p. 117-120.
31. Zhang, S. Shrestha, S.J. Huang, P. Aliberti, M.A. Green, and G. Conibeer, *Structural studies of multilayered Ge nanocrystals embedded in matrix fabricated using magnetron sputtering*. Energy Procedia, 2010. **2**(1): p. 243-250.

32. Teo, X.H. Sun, T.F. Hung, X.M. Meng, N.B. Wong, and S.T. Lee, *Precision-Cut Crystalline Silicon Nanodots and Nanorods from Nanowires and Direct Visualization of Cross Sections and Growth Orientations of Silicon Nanowires.* Nano Letters, 2003. **3**(12): p. 1735-1737.
33. A. Biswas, S. Bayer, A. Biris, T. Wang, E. Dervishi, F. Faupel, Advances in top–down and bottom–up surface nanofabrication: Techniques, applications and future prospects, Vol 170, Issues 1–2, 15 January 2012, Pages 2–27
34. Li, S.H. Chen, and H.L. Chen, *Thermal-flow techniques for sub-35nm contact-hole fabrication using Taguchi method in electron-beam lithography.* Microelectron. Eng., 2009. **86**(11): p. 2170-2175.
35. Guo, E. Leobandung, L. Zhuang, and S.Y. Chou, *Fabrication and characterization of room temperature silicon single electron memory.* Journal of Vacuum Science & Technology B: Microelectronics and Nanometer Structures, 1997. **15**(6): p. 2840-2843.
36. Moliton, *Solid-State Physics for Electronics*. 2009: John Wiley & Sons.
37. Harrison, *Quantum wells, wires, and dots: theoretical and computational physics*. 2000: John Wiley & Sons.
38. Schmid, G., *Nanoparticles: from theory to application*. 2004: Wiley-VCH.
39. Fox, *Optical properties of solids*. 2010: Oxford University Press.
40. Germanenko, S. Li, S.J. Silvers, and M.S. El-Shall, *Characterization of silicon nanocrystals and photoluminescence quenching in solution.* Nanostructured Materials, 1999. **12**(5-8): p. 731-736.
41. Yu, X. Wang, W. Lu, S. Wang, Y. Bian, and G. Fu, *Effects of substrate temperature on microstructural and photoluminescent properties of nanocrystalline silicon carbide films.* Physica B: Condensed Matter, 2010. **405**(6): p. 1624-1627.
42. Nayfeh, L. Mitas, *Silicon Nanoparticles: New Photonic and Electronic Material at the Transition Between Solid and Molecule*, in *Nanosilicon*, K. Vijay, Editor. 2008, Elsevier: Amsterdam. p. 1-78.
43. Eberl, O.G. Schmidt, O. Kienzle, and F. Ernst, *Preparation and optical properties of Ge and C-induced Ge quantum dots on Si.* Thin Solid Films, 2000. **373**(1-2): p. 164-169.
44. Chiquito, Y.A. Pusep, S. Mergulhão, J.C. Galzerani, and N.T. Moshegov, *Investigation of the InAs/GaAs self-assembled quantum dots using the*

relationship between the capacitance and the density of states. Physica E: Low-dimensional Systems and Nanostructures, 2001. **9**(2): p. 321-325.

45. Dolino, D. Bellet, *Variations in the lattice parameter of porous silicon produced by wetting and vapour adsorption.* Thin Solid Films, 1995. **255**(1-2): p. 132-134.

46. Charvet, R. Madelon, R. Rizk, B. Garrido, O. González-Varona, M. López, A. Pérez-Rodríguez, and J.R. Morante, *Substrate temperature dependence of the photoluminescence efficiency of co-sputtered Si/SiO_2 layers.* Journal of Luminescence, 1998. **80**(1-4): p. 241-245.

47. Rebohle, J. von Borany, W. Skorupa, I.E. Tyschenko, and H. Fröb, *Photoluminescence and electroluminescence investigations at Ge-rich SiO2 layers.* Journal of Luminescence, 1998. **80**(1-4): p. 275-279.

48. Ma, L. Wang, K. Chen, W. Li, L. Zhang, Y. Bao, X. Wang, J. Xu, X. Huang, and D. Feng, *Blue light emission in nc-Si/$_{SiO2}$ multilayers fabricated using layer by layer plasma oxidation.* Journal of Non-Crystalline Solids, 2002. **299-302**(Part 1): p. 648-652.

49. Crupi, D. Corso, S. Lombardo, C. Gerardi, G. Ammendola, G. Nicotra, C. Spinella, E. Rimini, and M. Melanotte, *Memory effects in MOS devices based on Si quantum dots.* Materials Science and Engineering: C, 2003. **23**(1-2): p. 33-36.

50. Xiaoli, S. Yi, G. Shulin, Z. Jianmin, Z. Youdou, S. Kenichi, I. Hiroki, and H. Toshiro, *Effects of interface traps in silicon-quantum-dots-based memory structures.* Physica E: Low-dimensional Systems and Nanostructures, 2000. **8**(2): p. 189-193.

51. Puglisi, S. Lombardo, G. Ammendola, G. Nicotra, and C. Gerardi, *Imaging of Si quantum dots as charge storage nodes.* Materials Science and Engineering: C, 2003. **23**(6-8): p. 1047-1051.

52. Lombardo, S. Coffa, C. Bongiorno, C. Spinella, E. Castagna, A. Sciuto, C. Gerardi, F. Ferrari, B. Fazio, and S. Privitera, *Correlation of dot size distribution with luminescence and electrical transport of Si quantum dots embedded in SiO_2.* Materials Science and Engineering B, 2000. **69-70**: p. 295-298.

53. Chen, Y. Ren, R.l. Xiong, Y.y. Zhao, and M. Lu, *Modulation of the photoluminescence of Si quantum dots by means of CO_2 laser pre-annealing.* Applied Surface Science, 2010. **256**(16): p. 5116-5119.

54. Reinig, B. Selle, F. Fenske, W. Fuhs, V. Alex, and M. Birkholz, *Highly oriented growth of polycrystalline silicon films on glass by pulsed magnetron sputtering*. Vol. 20. 2002: AVS. 2004-2006.

55. Torchynska, *Photoluminescence of Si nanocrystallites in different types of matrices.* Journal of Non-Crystalline Solids, 2006. **352**(23-25): p. 2484-2487.

56. Torchynska, T., J. Aguilar-Hernandez, M. Morales Rodriguez, C. Mejia-Garcia, G. Contreras-Puente, F.G. Becerril Espinoza, B.M. Bulakh, L.V. Scherbina, Y. Goldstein, A. Many, and J. Jedrzejewski, *Comparative investigation of photoluminescence of silicon wire structures and silicon oxide films.* Journal of Physics and Chemistry of Solids, 2002. **63**(4): p. 561-568.

57. Papon, J. Leblond, and P.H.E. Meijer, *The physics of phase transitions: concepts and applications*. 2006: Springer-Verlag.

58. Myerson, R. Ginde, *Crystals, crystal growth, and nucleation*, in *Handbook of Industrial Crystallization (Second Edition)*, S.M. Allan, Editor. 2002, Butterworth-Heinemann: Woburn. p. 33-65.

59. Spaepen, *Homogeneous Nucleation and the Temperature Dependence of the Crystal-Melt Interfacial Tension*, in *Solid State Physics*, E. Henry and T. David, Editors. 1994, Academic Press. p. 1-32.

60. Salk, D.E. Hagen, and C.K. Lutrus, *Propensity rule in homogeneous nucleation processes.* Chemical Physics Letters, 1988. **146**(6): p. 605-608.

61. Rao, B.J. Berne, *Nucleation in finite systems: Theory and computer simulation.* Astrophysics and Space Science, 1979. **65**(1): p. 39-46.

62. Mullin, *Nucleation*, in *Crystallization (Fourth Edition)*. 2001, Butterworth-Heinemann: Oxford. p. 181-215.

63. Cao, *Nanostructures & nanomaterials: synthesis, properties & applications*. 2004: Imperial College Press.

64. Idrees, F.A., S. Sakrani, and Z. Othaman, *Formation and Characterization of Silicon Self-assembled Nanodots.* AIP Conference Proceedings, 2011. **1341**(1): p. 324-327.

65. Priester, C. and M. Lannoo, *Growth aspects of quantum dots.* Current Opinion in Solid State and Materials Science, 1997. **2**(6): p. 716-721.

66. Le Thanh, V. and V. Yam, *Superlattices of self-assembled Ge/Si(0 0 1) quantum dots.* Applied Surface Science, 2003. **212-213**: p. 296-304.

67. Larsson, A. Elfving, P.O. Holtz, G.V. Hansson, and W.X. Ni, *Luminescence study of Si/Ge quantum dots.* Physica E: Low-dimensional Systems and Nanostructures, 2003. **16**(3-4): p. 476-480.

68. Talalaev, G.E. Cirlin, A.A. Tonkikh, N.D. Zakharov, P. Werner, U. Gösele, J.W. Tomm, and T. Elsaesser, *Miniband-related 1.4-1.8 [mu]m Luminescence of Ge/Si Quantum Dot Superlattices*, in *Handbook of Self Assembled Semiconductor Nanostructures for Novel Devices in Photonics and Electronics*, H. Mohamed, Editor. 2008, Elsevier: Amsterdam. p. 324-345.

69. Müller, O. Kirfel, A. Rastelli, H. von Känel, and D. Grützmacher, *Successful shape-preservation of Ge-clusters during Si-coverage at low temperature.* Materials Science and Engineering B, 2003. **101**(1-3): p. 142-145.

70. Zhou, R.A. Johnson, and H.N.G. Wadley, *Vacancy formation during vapor deposition.* Acta Materialia, 1997. **45**(11): p. 4441-4452.

71. Wood, *Thin-film optical filters: 3rd edition : H.A. Macleod; Thin Film Centre Inc., Tuscon, Arizona & University of Arizona, USA, Institute of Physics Publishing, 2001, 672pp, ISBN 0-7503-0688-2.* Optics and Lasers in Engineering, 2002. **37**(6): p. 673-674.

72. Palmero, H. Rudolph, and F.H.P.M. Habraken, *One-dimensional analysis of the rate of plasma-assisted sputter deposition*. Vol. 101. 2007: AIP. 083307.

73. Margaritondo, R. Joynt, M. Onellion, and A.V. Society, *High Tc superconducting thin films, devices, and applications, Atlanta, GA, 1988*. 1989: American Institute of Physics.

74. Bach, D. Krause, *Thin films on glass*. 1997: Springer.

75. Shi, *Functional thin films and functional materials: new concepts and technologies*. 2003: Springer.

76. Mattox, *Physical Sputtering and Sputter Deposition (Sputtering)*, in *Handbook of Physical Vapor Deposition (PVD) Processing (Second Edition)*. 2010, William Andrew Publishing: Boston. p. 237-286.

77. Mattox, *Film Characterization and Some Basic Film Properties*, in *Handbook of Physical Vapor Deposition (PVD) Processing*. 1998, William Andrew Publishing: Westwood, NJ. p. 569-615.

78. Mattox, *Vacuum Evaporation and Vacuum Deposition*, in *Handbook of Physical Vapor Deposition (PVD) Processing*. 1998, William Andrew Publishing: Westwood, NJ. p. 288-342.

79. Behrisch, W. Eckstein, *Sputtering by particle bombardment: experiments and computer calculations from threshold to MeV energies*. 2007: Springer.

80. Behrisch, K. Wittmaack, *Sputtering by particle bombardment III: characteristics of sputtered particles, technical applications*. 1991: Springer-Verlag.

81. Hattum, A.P. , H.R. W. M. Arnoldbik, and F.H.P.M. Habraken, *Distinct processes in radio-frequency reactive magnetron plasma sputter deposition of silicon suboxide films.* Journal of applied physics, 2007(124505): p. 102.

82. Licari, L.R. Enlow, *Thin Film Processes*, in *Hybrid Microcircuit Technology Handbook (Second Edition)*, J.L. James and R.E. Leonard, Editors. 1998, William Andrew Publishing: Westwood, NJ. p. 63-103.

83. Kodigala, K. Subba Ramaiah, *Structural Properties of I-III-VI2 Absorbers*, in *Thin Films and Nanostructures*. 2010, Academic Press. p. 115-194.

84. Benchiheb, M.S. Aida, and N. Attaf, *Plasma optical emission spectroscopy diagnostic during amorphous silicon thin films deposition by Rf sputtering technique.* Materials Science and Engineering: B, 2010. **172**(2): p. 191-195.

85. Allen, D.J. Tildesley, *Computer Simulation of Liquids*. 1989: Oxford University Press, USA.

86. S. Sakrani, L.Qie.Jie, Yussof Wahab, *The formation of nanoscale clusters – nanofilms / quantum dots predicted using a capillary model of nucleation.* Journal of Fundamental Sciences, 2005: p. 23-34.

87. Madras, B.J. McCoy, *Temperature effects on the transition from nucleation and growth to Ostwald ripening.* Chemical Engineering Science, 2004. **59**(13): p. 2753-2765.

88. Qin, *Bubble formation in lattice Boltzmann immiscible shear flow.* The Journal of Chemical Physics, 2007. **126**(11): p. 114506-5.

89. M. Ali, *Growth and study of magnetostrictive FeSiBC thin films for device applications*, in *Department of Physics & Astronomy*. 1999, The University of Sheffield.

90. Birkholz, P.F. Fewster, and C. Genzel, *Thin film analysis by X-ray scattering*. 2006: Wiley-VCH.

91. Birkholz, *Principles of X-ray Diffraction*, in *Thin Film Analysis by X-Ray Scattering*. 2006, Wiley-VCH Verlag GmbH & Co. KGaA. p. 1-40.

92. Cullity, S.R. Stock, *Elements of x-ray diffraction*. 2001: Prentice Hall.

93. Samavati, A., F. Aldaw, S.K. Ghoshal, Z. Othaman, and S. Sakrani, *Light emitting germanium and silicon nanoislands grown by RF magnetron sputtering.* Journal of Ovonic Research. **8**(3): p. 65-72.

94. Chen, Z. Jiao, M.H. Wu, C.H. Shek, C.M.L. Wu, and J.K.L. Lai, *Microstructural evolution of oxides and semiconductor thin films.* Progress in Materials Science, 2011. **56**(7): p. 901-1029.

95. Hasegawa, M. Sakata, T. Inokuma, and Y. Kurata, *Structural change of polycrystalline silicon films with different deposition temperature.* Journal of applied physics, 1999. **85**(7): p. 3844-3849.

96. Setyawan, M. Shimada, Y. Imajo, Y. Hayashi, and K. Okuyama, *Characterization of particle contamination in process steps during plasma-enhanced chemical vapor deposition operation.* Journal of Aerosol Science, 2003. **34**(7): p. 923-936.

97. Mattox, *5 - Vacuum Evaporation and Vacuum Deposition*, in *Handbook of Physical Vapor Deposition (PVD) Processing*. 1998, William Andrew Publishing: Westwood, NJ. p. 288-342.

98. De Los Santos, D. Lee, J. Seo, F.L. Leon, D.A. Bustamante, S. Suzuki, Y. Majima, T. Mitrelias, A. Ionescu, and C.H.W. Barnes, *Crystallization and surface morphology of Au/SiO2 thin films following furnace and flame annealing.* Surface Science, 2009. **603**(19): p. 2978-2985.

99. Chen, L. Lai, C.H. Shek, and H.D. Chen, *Production of amorphous tin oxide thin films and microstructural transformation induced by heat treatment.* Applied Physics A: Materials Science & Processing, 2005. **81**(5): p. 1073-1076.

100. Sun, H.C. Kang, *Synthesis and characterization of self-assembled ZnO nano-dots grown on SiNx/Si(001) substrates by radio frequency magnetron sputtering*. Thin Solid Films. **518**(22): p. 6522-6525.

101. Germanenko, *Effect of atmospheric oxidation on the electronic and photoluminescence properties of silicon nanocrystals.* Pure Appl. Chem, 2000, Vol. 72, Nos. 1–2, pp. 245–255.

102. Chen, H. Chang, A.-T. Chou, T.-M. Hsu, P.-S. Chen, Z. Pei, and L.-S. Lai, *Optical properties of stacked Ge/Si quantum dots with different spacer thickness grown by chemical vapor deposition.* Applied Surface Science, 2004. **224**(1-4): p. 148-151.

103. Gfroerer, *Photoluminescence in Analysis of Surfaces and Interfaces*, in *Encyclopedia of Analytical Chemistry*. 2006, John Wiley & Sons, Ltd.

104. Kenyon, P. Trwoga, C.W. Pitt, and G. Rehm, *The origin of photoluminescence from thin films of silicon-rich silica.* Journal of applied physics, 1996. **79**(12): p. 9291-9300.

105. Ma, L. Wang, K. Chen, W. Li, L. Zhang, Y. Bao, X. Wang, J. Xu, X. Huang, and D. Feng, *Blue light emission in nc-Si/SiO_2 multilayers fabricated using layer by layer plasma oxidation.* Journal of Non-Crystalline Solids, 2002. **299-302, Part 1**(0): p. 648-652.

106. Chen, Z. Ma, X. Huang, J. Xu, W. Li, Y. Sui, J. Mei, and D. Zhu, *Comparison between light emission from Si/SiNX and Si/SiO_2 multilayers: role of interface states.* Journal of Non-Crystalline Solids, 2004. **338-340**(0): p. 448-451.

107. Zheng, Y.H. Zuo, W. Wang, Y.L. Tao, C.L. Xue, B.W. Cheng, and Q.M. Wang, *Efficient emission and energy transfer in Si/Er-Si-O multilayer structure.* Materials Research Bulletin, 2011. **46**(2): p. 262-265.

108. Fafard, Ventra, Massimiliano, Evoy, Stephane Heflin, James, *Quantum-Confined Optoelectronic Systems Introduction to Nanoscale Science and Technology*. 2004, Springer US. p. 443-483.